Final Technical Report

U.S. Geological Survey National Hazards Reduction Program (NEHRP)

Influence of sediment dynamics and alluvial fan formation on paleoseismic studies in southern California, North America

Sourav Saha [1]

Seulgi Moon [2]

Nathan Brown [3]

[1] Department of Earth, Planetary, and Space Sciences, University of California Los Angeles, 595 Charles E Young Dr. E, Los Angeles, CA 90095

Fax: none

Email: sahasv@mail.uc.edu

[2] Department of Earth, Planetary, and Space Sciences, University of California Los Angeles, 595 Charles E Young Dr. E, Los Angeles, CA 90095

Fax: none

Email: sgmoon@ucla.edu

[3] Department of Earth and Environmental Sciences, University of Texas at Arlington, 107 Geoscience Building, 500 Yates Street, Arlington, Texas 76019

Fax: none

Email: nathan.brown@uta.edu

Grant Award No. G20AP00044

Award term: 03/15/2020–03/14/2021

Research supported by the U.S. Geological Survey (USGS), Department of Interior, under USGS award number G20AP00044. The views and conclusions contained in this document are those of the authors and should not be interpreted as necessarily representing the official policies, either expressed or implied, of the U.S. Government.

TABLE OF CONTENTS

Abstract ……..…….. 3

Report ……...…….…….. 3

Introduction ……..… 3

Methods ……..…. 7

Sample collection and preparation ……..….. 7

Luminescence measurements and age determination ……..….. 9

Depositional history from single-grain luminescence subpopulation ages ……..……. 10

Dating results from seven nested alluvial fans ……..….. 11

Discussions ……..... 12

Depositional events in the upper Mission Creek catchment …… 12

Sediment reworking and mixing ……..…. 17

Conclusions …… 17

Appendix 1 – Luminescence age analysis ……...……...… 18

Acknowledgments ……..…. 20

Project data ……. 20

Bibliography of publications resulting from the work performed under this award …….. 20

References …….. 21

ABSTRACT

Significant sediment flux and deposition in a sedimentary system are influenced by climate changes, tectonics, lithology, and the sedimentary system's internal dynamics. Since sedimentary records are often spatially and/or temporally incomplete, identifying the timing of significant depositional periods from stratigraphic records is a first step to critically evaluating sediment flux and deposition controls. Here, we show that the ages of single-grain K-feldspar luminescence subpopulations may provide information on the timing of previous major depositional periods. We analyzed >700 K-feldspar single-grains from 12 samples from the surface to ~1-m-depth in seven sub-sequences of alluvial fan surfaces in the upper Mission Creek catchment of southern California. Single-grain luminescence subpopulation ages from seven different pits significantly overlap at least twelve times since ~100 ka indicating a common depositional history. The lower and upper Mission Creek depositional periods correspond reasonably well with the late Pleistocene and Holocene intervals of wetter than average climate conditions based on hydroclimatic proxies from nearby locations. Our findings imply a first-order climatic control on sediment depositional history in southern California on a millennial timescale.In addition, we find that some luminescence subpopulations ages are younger than independently dated fan surface ages from previous work, which suggests a potential grain mixing near the alluvical fan surface.

REPORT

1. Introduction

Paleoseismic event dating and slip rate measurements often assume simple geomorphic processes and complete stratigraphic preservation (e.g., Biasi et al., 2002). That is why sites with higher sedimentation rates are often preferred, assuming that sedimentary archives preserve their primary stratigraphy (Hempton et al., 1983) and record sufficiently large earthquake events or surface ruptures effectively. However, this assumption has rarely been tested. For example, sediment starvation or hiatus (or intense erosion) between earthquake events (e.g., lack of unconformities) could make multiple events appear as one event, and therefore add intrinsic biases in the interpretation of paleoseismic events, including estimates of average (apparent) recurrence intervals in the geologic past. Furthermore, since paleoseismic studies often rely on spatially and/or temporally incomplete stratigraphic sequences (Jerolmack & Paola, 2010; Miall, 2015) or suffer from poor chronological constraints (Owen et al., 2014 and references therein), it is, therefore, crucial to define the timing of significant sediment flux and deposition in a well-connected sediment routing system.

In addition, variations in external environmental perturbations such as climate and tectonics and intrinsic factors such as lithology and the sedimentary system's internal dynamics also influence sediment flux and deposition in a catchment (Romans et al., 2016; Toby et al., 2019). How these allogenic and autogenic signals are propagated downstream and accurately recorded (or shredded) in the geomorphic and stratigraphic archives over various geologic timescales is still poorly understood (Gray et al., 2019; Caracciolo et al., 2020). Due to the complexity of these various factors, it is challenging to identify the first-order control, whether external (allogenic) or

internal (autogenic), on sediment generation, transport, and downstream deposition (Armitage et al., 2011, 2013). For example, researchers still debate whether the significant alluvial fan depositions in the American Southwest took place during relatively dry periods, especially during glacial to interglacial transitions with reduced soil moisture and vegetation cover (e.g., Bull, 1977, 1991, 2000; Wells et al., 1987, 1990; Spelz et al., 2008) or during the wetter periods due to enhanced runoff and sediment transport capacity (e.g., Ponti, 1985; Harvey et al., 1999; Inman & Jenkins 1999; Warrick & Milliman 2003; Miller et al., 2010; Kirby et al., 2012, 2014; Owen et al., 2014; Ellwein et al., 2015).

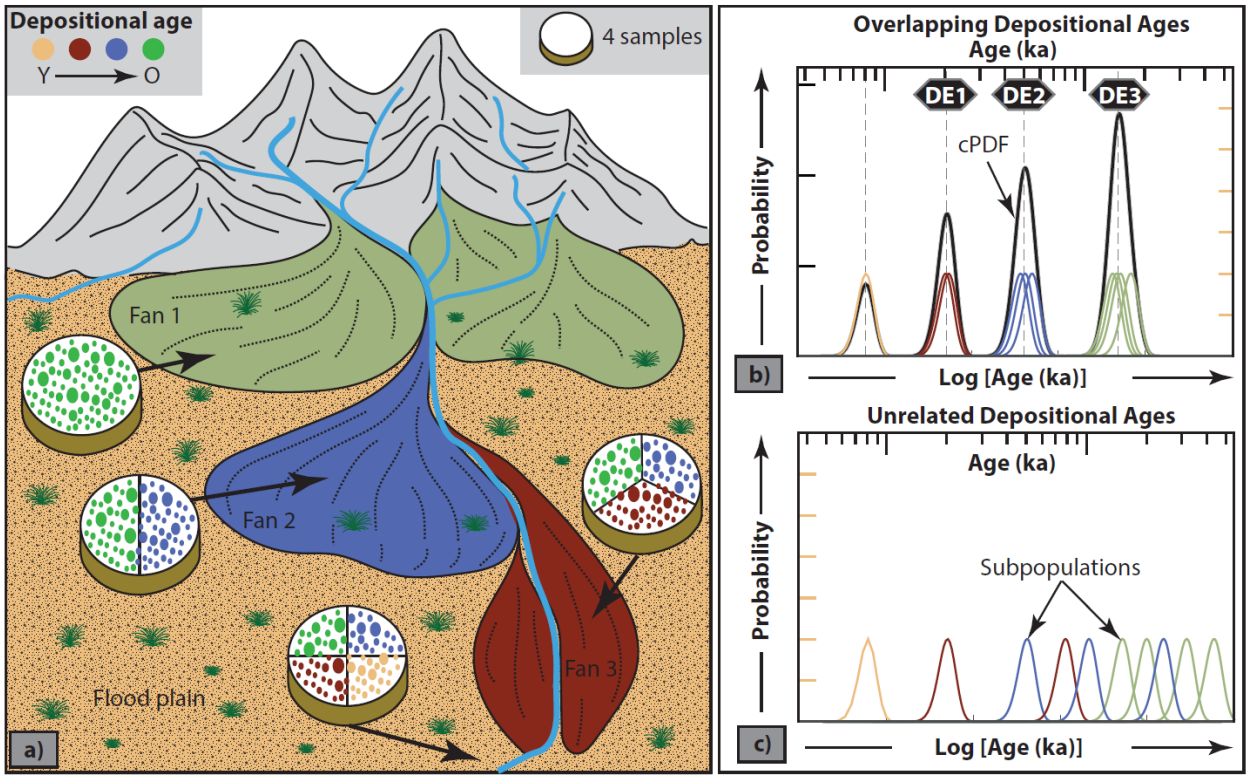

Figure 1. (a) *Schematic representation of a simplified sediment routing system and expected age distribution of single-grain luminescence subpopulations. Different colors of stippling mounted on discs represent multiple single-grain luminescence ages from three distinct fans and the floodplain (arrows show the sample's location). Ideally, different proportions of single-grain ages are expected if some grains experience unbleached transport before their burial and retain their previous luminescence signals.* ***(b)*** *A hypothetical example of three overlapping depositional events (i.e., DE1, DE2, and DE3, where D.E. is a depositional event) derived from ten subpopulations determined from four samples collected at distinct fans and the floodplain. This is expected if the subpopulations share common sediment depositional history. Composite probability (cPDF) is presented for the closely overlapping subpopulations (black line), with the dashed line highlighting the mode. The y-axes show probability corresponding to log[age(ka)] (Galbraith, 2011; see section 2.3). Note that 10% relative errors are used for the hypothetical single-grain subpopulations in log-scale, resulting in narrower cPDF peaks for older ages.* ***(c)*** *An alternative scenario where the subpopulations do not overlap at a specific time, likely indicating*

either unrelated or more complex site-specific stochastic depositional histories or extensive partial bleaching of the luminescence signals in most single grains. This figure and the caption are from Saha et al., in press.

Single-grain luminescence signals can be used effectively to examine variable past sunlight exposure (luminescence bleaching) and burial (luminescence regeneration) history (Arnold et al., 2007; Smedley et al., 2015; Gray et al., 2018, 2019; Saha et al., *in press*). Before burial, some grains may experience sunlight exposure during transport, and their luminescence clock is reset to zero (Rhodes, 2011). However, other grains may have experienced no or limited sunlight exposure during transport depending on transport conditions or bleachability of the targeted luminescence signal (e.g., feldspar signals bleach slower than quartz signals) (Colarossi et al., 2015; Gray et al., 2019; Brown, 2020). For example, a grain traveling within turbulent, muddy water may experience very dim attenuated sunlight. In contrast, windblown grains often see a bright, full spectrum of sunlight. In addition, for feldspar grains in fluvial settings, complete signal resetting of all grains prior to burial is not guaranteed (Wallinga, 2002; Gliganic et al., 2017; Brill et al., 2018). In this case, the recorded luminescence signals and age distribution of feldspar grains can provide information on the past sediment depositional history (e.g., Gliganic et al., 2015, 2016; Rhodes, 2015; Saha et al., *in press*).

Figure 1a presents a simple schematic of nested alluvial fans and a floodplain depositional setting. We can assume a situation where a fraction of feldspar grains is well-bleached during any single flood, and a negligible fraction of grains is partially bleached. In contrast, most other grains experience unbleached transport before subsequent burial events and retain luminescence signals from prior burial events. In that case, we can use the multiple ages of single-grain subpopulations (i.e., different colors of stippling in discs representing multiple single-grain ages in Figure 1a) to estimate the most recent and previous depositional events. If a sedimentary system is driven by significant external environmental perturbation, large burial events may be preserved in distant deposits in multiple stratigraphic units in a well-connected sediment routing system (Figure 1b). As such, single-grain luminescence subpopulation ages from different deposits are expected to show multiple overlapping ages likely driven by the shared perturbations (e.g., DE1, DE2, and DE3 events in Figure 1b; Saha et al., *in press*). However, if autogenic processes dictate sediment transport or extensive partial bleaching occurs for most grains, single-grain subpopulation ages from different deposits may produce unrelated ages without any tight overlapping and are not associated with any shared perturbations (Figure 1c; Saha et al., *in press*).

To test this hypothesis, we examine luminescence ages in single-grain K-feldspars using the post-Infrared Infrared Stimulated Luminescence (p-IR IRSL; Reimann et al., 2012; Rhodes, 2015) technique from deposits in the upper and lower Misson Creek catchment. In a trench located downstream of the Mission Creek catchment, we analyzed 17 samples from the surface to ~9 m-depth. This work is partially supported by this grant and is published in Saha et al. (*in press*). In addition, we dated twelve sediment samples from the surface (~0.3 m) to ~1 m depth from seven different pits at seven different nested alluvial fan surfaces in the upper Mission Creek, southern California. These ages were compared with independently dated ages using ^{10}Be in previous

studies (e.g., Owen et al., 2014) (Figure 2). We plan to submit a paper based on these results soon (Saha et al., *in prep*). This report is based on both Saha et al. (in press) and Saha et al. (in prep).

In these works, we first identified significant depositional periods shared in multiple samples collected from distinct stages of alluvial fan surfaces. Then, we compared these upstream depositional periods with the downstream depositional events in the lower Mission Creek on the Banning strand of the San Andreas Fault (SAF) and with the regional hydroclimatic proxies from nearby sites in southern California.

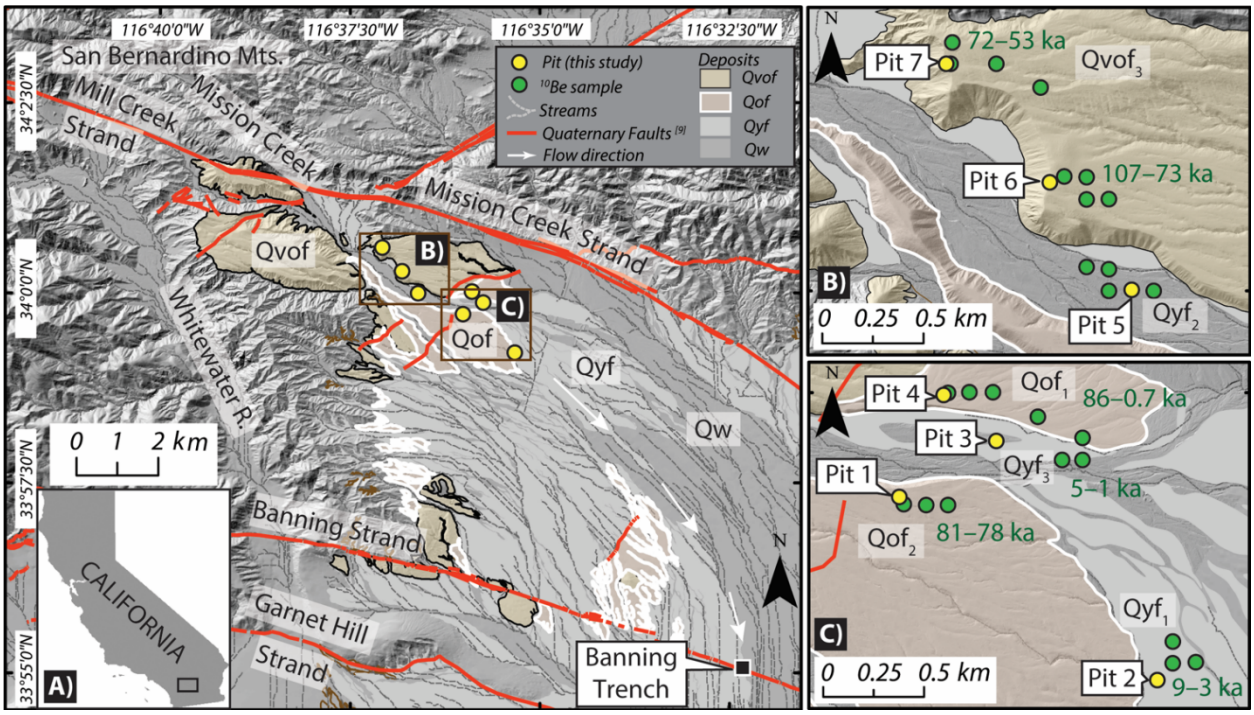

Figure 2. A) *The surficial deposit and fault map of the Mission Creek catchment modified after the Quaternary geological map of southern California (e.g., Lancaster et al., 2012; Kendrick et al., 2015) and the Quaternary Fault and Fold Database of the United States (Hart et al., 2001), respectively. The surficial deposit map is superimposed on a hillshade map generated from the LiDAR Digital Elevation Model (DEM) (USGS). Three primary sequences of nested alluvial fans (Qvof, Qof, Qyf) at the upper Mission Creek catchment are shown along with recalculated* ^{10}*Be ages (green circle) (Owen et al., 2014). The downstream trench site on the Banning strand is also shown. Seven ~1-m deep pits (yellow circle) were dug to collect luminescence samples.* ***B)*** *and* ***C)*** *exhibit the enlarged fan sequences with pit locations,* ^{10}*Be sample location, and* ^{10}*Be age range. The fan's sub-sequences are indicated by the subscript numbers, where a lower value means the older fan.*

In addition, we compared the published ^{10}Be surface boulder and depth profile ages from different nested alluvial fan surfaces with the new luminescence data from multiple samples at the upper Mission Creek to assess the accuracy and uncertainties of the two independent dating techniques (Figure 2). Our results show potential grain mixing at the surface for alluvial fans older than ~1 ka. Our work show that significant alluvial depositions occurred during the intervals of

wetter than average hydroclimate conditions in the Mission Creek catchment in southern California.

2. Methods

2.1. Sample collection and preparation

The upper Mission Creek catchment represents a classic range-front semi-arid sequential alluvial fan setting (e.g., Bowman, 1978; Colombo, 2005), with at least three primary and eight sub-sequences of alluvial fans (Figure 3; Matti & Cossette, 2007; Owen et al., 2014; Kendrick et al., 2015; Matti et al., 2015; Fosdick & Blisniuk, 2018). Nineteen sediment samples were collected from ~1 m-deep pits from these seven sub-sequences of alluvial fan surfaces, 2–3 samples from each pit (Figure 4). We dated twelve samples from these fans—2 samples from each fan, except Pit 6 and 7, which were dug at the oldest Quaternary fan surfaces (Qvof3). Approximately 10 km downstream from Pit 3, a paleoseismic trench was previously excavated on the Banning strand of SAF at the lower Mission Creek (Castillo et al., 2021). Seventeen luminescence samples were dated from this trench (Saha et al., *in press*). We followed the similar sampling procedure and protocol in this study and compared the published luminescence ages (Saha et al., *in press*) with the new data generated from this study (Figure 5).

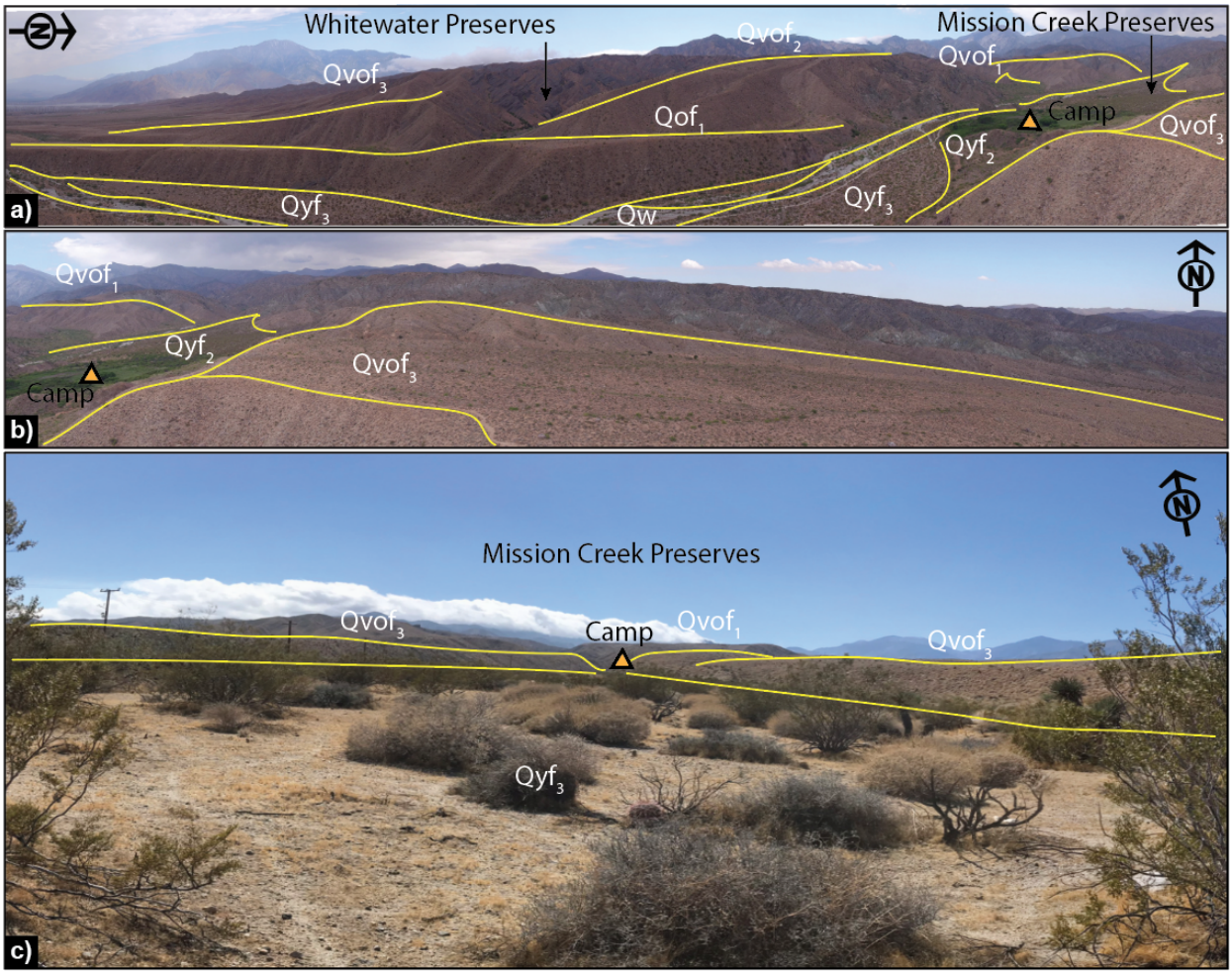

Figure 3. *Upper Mission Creek sequence alluvial fans. The campsite is shown for a relative comparison of the photographs.* ***a)*** *UAV photo of the westside of the fan; view looking west/northwest.* ***b)*** *UAV footage of the eastside of the fan; view looking north.* ***c)*** *View looking upstream fans. Three primary sequences (i.e., Qvof, Qof, Qyf) and as many as eight sub-sequences (i.e., $Qvof_1$, $Qvof_2$, $Qvof_3$, Qof_1, Qof_2, Qyf_1, Qyf_2, Qyf_3; where the lower subscript number indicates the older fan) of nested Quaternary alluvial fans are identified in the field and annotated after Matti and Cossette (2007), Owen et al. (2014), and Kendrick et al. (2015).*

The pit exposures mainly consist of matrix-supported massive sandy units with cobbles, pebbles, and boulders, indicating possibly high energy deposition. We did not see any layering or stratification in any of our pits. Soil development in all the fan surfaces is poor, with reddish color in the oldest Quaternary fan surfaces (Qvof in Figure 4a, c) and grayish color for the rest of the nested fans (Qof and Qyf in Figure 4d, e). The presence of large boulders below ~1-m precludes us from collecting samples at depths larger than 1-m. Although we selected pits with no evidence of bioturbations (Figure 2b, c), signs of extensive bioturbation at the fan surfaces are often more common in this semi-arid setting.

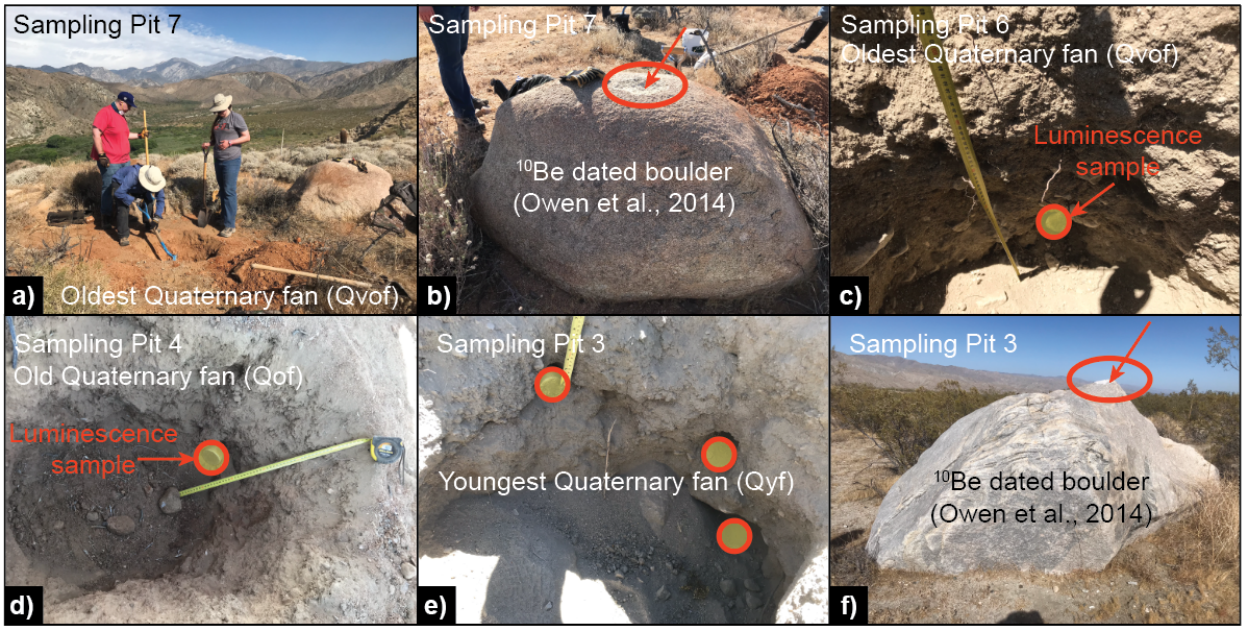

Figure 4. *Field photos showing the ~1-m-deep pits, luminescence sample collection, and a previously ^{10}Be dated alluvial fan surface boulders.* ***a)*** *Pit 7 was dug close to one of the ^{10}Be dated surface boulders* ***(b)*** *at the oldest Quaternary alluvial fan ($Qvof_3$). Luminescence sample locations for pit 6* ***(c)*** *and 4* ***(d)*** *at the oldest ($Qvof_3$) and old Quaternary alluvial fan surfaces (Qof_2) are shown.* ***e)*** *Pit 3, the youngest Quaternary alluvial fan (Qyf_3), is also excavated near one of the ^{10}Be dated surface boulders* ***(f)****.*

An opaque 5 cm-diameter tube was pushed horizontally into freshly cleaned walls at each sample pit and capped immediately to protect from sunlight (Figure 4c, d, e). We isolated K-feldspar grains at the UCLA Luminescence Laboratory following the procedure of Rhodes (2015)

under dim amber LED light conditions. We performed wet sieving to extract suitable grain sizes (175–200 µm), followed by drying. The 175–200 µm grain sizes were then treated with a lithium metatungstate (LMT) solution of 2.565 g cm^{-3} to isolate the most potassic (k) feldspar fraction (the "Super-K" procedure in Rhodes, 2015). The Super-k fraction was further sieved one more time to remove any broken finer grains. This procedure was shown to increase the net IRSL sensitivity by a factor of ~100 (see Rhodes, 2015; McGuire & Rhodes, 2015). Grains were then visually investigated under a binocular microscope to check for any coatings. We did not observe any unusual coatings. Since HF treatment (e.g., 10% silica-saturated HF for 10 min; Rhodes, 2015) for feldspar grains may induce very irregular etching and likely does not remove surface uniformly (e.g., Bell 1980; Brennan et al., 1991), we preferred not to apply the HF treatment. We determined the field water content for each sample from their weights before and after drying.

2.2. Luminescence measurements and age determination

We carried out the p-IR IRSL measurements using a TL-DA-20 Risø automated reader equipped with a single-grain I.R. laser (830 nm, at 90% of 150 mW; Bøtter-Jensen et al., 2003). Emissions were detected using an EMI 9235QB photomultiplier tube fitted with a BG3 and BG39 filter combination, allowing transmission around 340–470 nm. A single-grain post-Infrared Infrared Stimulated Luminescence single-aliquot regenerative-dose protocol (p-IR IRSL SAR protocol; Buylaert et al., 2009; Rhodes, 2015) was used to measure the equivalent dose (De) values for individual grains. Samples were preheated at 250°C for 60s before natural and regenerative measurements, and a stimulation temperature of 50°C and 225°C was used to estimate equivalent doses (De). The SAR dose-response curves were used to measure the total radiation dose required to produce the natural luminescence signal (i.e., the equivalent dose, De; Murray & Wintle, 2000). We calculated the De without applying any rejection criteria to capture the behaviors of all grains.

We measured the *in-situ* gamma dose rate using a portable NaI gamma spectrometer. The elemental concentrations of U and Th were measured with inductively-coupled plasma mass spectrometry (ICP-MS), and the K concentration was measured using inductively-coupled plasma optical emission spectrometry (ICP-OES). These values were used to calculate the total beta dose-rate contribution using Liritzis et al.'s (2013) conversion factors. A value of 12.5 ± 0.5 wt.% K content was used in calculating the internal beta dose rate (Huntley & Baril, 1997). Although this internal K content value is likely on the higher end (Smedley et al., 2012; Smedley & Pierce, 2016), they generally produce consistent apparent ages that often show good agreement with independent dating methods (particularly with ^{14}C and ^{10}Be in Rhodes, 2015). Since most of our K-feldspar grains give bright p-IR IRSL signals and we did not directly measure the internal K content, we decided to use this value of 12.5 ± 0.5 wt.% K for the age analysis. The alpha dose rate was also estimated using the conversion factors of Liritzis et al. (2013). An alpha attenuation factor from Brennan et al. (1991) and a beta attenuation factor from Guerin et al. (2012) were used. The cosmic ray contribution was derived from the sample's burial depth, latitude, and altitude (Prescott & Hutton, 1994).

We calculated the environmental dose rate and p-IR $IRSL_{225}$ ages (± 1σ standard error) for individual grains using the DRAC v1.2 online calculator (Durcan et al., 2015), assuming a constant

radiation dose environment and field moisture content. All twelve samples show an extremely high degree of dispersion between single-grain De (OD of 46–179%), suggesting heterogeneous bleaching of feldspar grains. We used the semi-parametric three-parameter finite mixture model (FMM), assuming an OD of 15% to model the ages of single-grain subpopulations (imposing k age components) (e.g., Saha et al., *in press*). By minimizing the Bayesian Information Criterion (BIC) score from FMM results, one can estimate the most probable number of age components within a population and estimates the age ± 1σ standard error for each component assuming that each component has a Gaussian distribution (hereafter FMM-subpopulations) (Figure 5b; Galbraith & Green, 1990; Galbraith & Laslett, 1993; Galbraith, 2005). We used the R statistical package (Kreutzer et al., 2012) to perform FMM. Applying FMM is appropriate for identifying distinct subpopulations considering that the average relative standard error of single-grain ages in this dataset is ~10% (e.g., Brandon, 1992). We also tested for the presence of athermal fading (Huntley & Lamothe, 2001) for timescales ranging from ~300 seconds to 7 days (Figure A1).

2.3. Depositional history from single-grain luminescence subpopulation ages

To examine the distribution of single-grain subpopulation ages in all samples collected from distinct fan surfaces, we calculated individual and composite probability (cPDF) distributions of FMM-subpopulations (Figures 5a, b, A2a, b) (Saha et al., *in press*). The cPDF was calculated by summing PDFs of all FMM-subpopulations. However, the potential of recording past subpopulation ages for each sample is restricted to the age ranges older than its most recent depositional age (Figure A2c; Saha et al., *in press*). Thus, the cPDF for a given age interval was normalized by the total number of samples available for that age interval (Figure A2c; Saha et al., *in press*). This normalized cPDF shows the relative probability density distribution of depositional ages corrected for a sample's availability (hereafter, relative cPDF). For reference, we also showed (1) the number of samples that can provide the record (henceforth, available samples), (2) the number of samples whose 2σ range overlap (hereafter, overlapping samples), and (3) the fraction of overlapping samples relative to available samples that vary with the given age interval (Figure A2c).

In addition, since older ages tend to have larger absolute errors than younger ages (i.e., as age increases, uncertainty increases) (e.g., Berger 2010, 2011; Ivy-Ochs et al., 2007), the probability distribution for older ages often exhibit subdued modal heights (Figure A2a). The opposite is true for young ages with high precision, often producing overly sharp peaks (Figure A2a). To minimize this bias, we plotted the individual and relative cPDF of FMM-subpopulation ages on a log scale with the corresponding relative probability, calculated based on the Jacobian transformation described in Galbraith (2011) (Figures 5a, b, A2b) (Saha et al., *in press*). Using a logarithmic scale of ages and corresponding probability makes it easier to identify multiple modes within the relative cPDF generated from distinctive clusters of FMM-subpopulation ages.

We then identified significant local maxima (modes) in the relative cPDF using the 'findpeaks' function in MATLAB's Signal Processing Toolbox (Figure 5a, b). We defined a peak where the minimum probability difference between a high probability point and neighboring troughs exceeds 5% of the full range of the relative cPDF, following the argument presented in Saha et al., *in press*.

The ages of local maxima identified in both relative cPDFs in linear and log scales are identical within 0.1 ka (Figure A2a, b). Any FMM age clusters comprised of <5% of single grains are considered less probable ages and are excluded from further analysis.

Finally, the upstream alluvial fan modal ages (this study) were compared with inferred downstream depositional periods on the Banning strand (Saha et al., *in press*) and selected (nearest) terrestrial hydroclimatic proxies. Our objective is to evaluate whether the timing of significant depositional periods is pervasive throughout the catchment and whether regional hydroclimatic variability plays a primary control in delivering and depositing sediments from upstream to downstream sections (Figure 5). Comparing the luminescence FMM-subpopulations ages (burial ages) with the published ^{10}Be data (exposure ages from boulders and a depth profile) from the same sites also offer insights into the geomorphic process uncertainties to these dating methods.

3. Dating results from seven nested alluvial fans

Although feldspar grains bleach more slowly, the p-IR $IRSL_{225}$ signals in all our samples are bright. We obtained a significant portion of well-behaved grains in all the samples. This helps to identify meaningful FMM-subpopulations. While, on average, none of the samples shows fading at 225°C during the laboratory experiment (e.g., Buylaert et al., 2009), there is a wide range of observed g-values for each sample with significant uncertainties (Figure A1). This is analogous to the previous study in the upper (Ataee, 2019) and lower Mission Creek catchment (Saha et al., *in press*). Thus, we did not apply fading corrections.

All twelve samples dated show OD ranging from ~46–179%, yielding much higher OD values than the 15% typical for well-bleached samples from southern California (Rhodes, 2015). Sixty FMM-subpopulations are identified from twelve samples (excluding FMMs with <5% single-grains), with notable overlap for at least twelve times (Figure 5b). The FMM-subpopulation ages of the nested fan surfaces range between ~0.3 and ~100.8 ka. We identify at least twelve prominent local maxima in the past ~100.0 ka from the relative cPDF of the IRSL data (Figures 5b, A2a, b). The modal ages that constitute those local maxima are ~100.8, ~44.5, ~26.6, ~17.8, ~13.5, ~6.2, ~3.1, ~1.6, ~1.3, ~0.8, and ~0.3 ka (Figure 5b). Three additional peaks at ~10.0, ~7.0, ~5.5 ka may also be seen with the individual FMM-subpopulation clusters (Figure 5b). However, due to overlapping errors, they fail to generate any modal distribution distinct from the ~13.5 and ~6.2 ka local maxima in the cPDF, respectively (Figures 5b, A2a, b).

We did not date the oldest $Qvof_1$ fan. However, it is dated to ~260 ka using ^{36}Cl/^{10}Be burial dating of alluvial sediments (Balco et al., 2019). When compared with the ^{10}Be depth profile age (~66 ka) of the $Qvof_2$ fan (Pit 6), we found a close correspondence with the 2nd highest proportion (29%) FMM-subpopulation age (~61 ka) of the sample J1582 (Figure 6). We also found that the youngest cluster of ^{10}Be surface boulder ages (~53 ka), which likely is the surface abandonment age of the $Qvof_3$ fan (Pit 7), match closely with the 2nd highest proportion (31%) FMM-subpopulation age (~57 ka) of the sample J1584 (Figure 6).

For the Qof_1 fan surface (Pit 1), the 2nd highest proportion (38%) FMM ages (~62 ka) of the samples J1569 and J1570 show close correspondence with the youngest ^{10}Be boulder ages (~78 ka) at ± 1σ (Figure 6). Similar correspondence between ^{10}Be boulder ages (~58 ka) and 2nd highest FMM-subpopulation (~64 ka) is also noticed for the Qof_2 fan surface (Pit 4) located on the eastern part of the Mission Creek (Figure 6).

For the younger Qyf1 (Pit 2) fan, similar age correspondence at ± 1σ can also be found between the youngest ^{10}Be boulder ages (~3.4 ka) and 2nd highest FMM-subpopulation (~3.2 ka; Figure 6). For the Qyf_2 fan (Pit 5), we found a corresponding youngest ^{10}Be boulder ages (~1.8 ka) and FMM-subpopulation age (~1.3–1.4 ka) at ± 1σ (Figure 6). However, the corresponding FMM-subpopulations in J1579 and J1581 do not contain a high proportion of grains (Figure 6). In contrast, the youngest FMM-subpopulation age (~0.8 ka) with the highest proportion of single-grans (20%) in the youngest Qyf_3 fan (Pit 3) matches reasonably well with the youngest ^{10}Be boulder age cluster (~1 ka; Figure 6). Except for the youngest (~1–0.8 ka) Qyf_3 fan surface samples (J1574, J1576), all other older surface sediment samples show several unusually young FMM-subpopulations (Figure 6).

4. Discussions

4.1. Depositional events in the upper Mission Creek catchment

We identify at least twelve prominent local maxima in the relative cPDF in the last ~100 ka, with the possibility of additional three local maxima, which likely represent the timing of significant depositional periods in the upper Mission Creek catchment, southern California (Figure 5b). These depositional periods include single local maximum during the Marine Isotope Stage (MIS) 5 (~100.8 ka), MIS 4 (~62.1 ka), MIS 3 (~44.5 ka), three local maxima during MIS 2 (~26.6, ~17.8, ~13.5 ka), and at least six (~6.2, ~3.1, ~1.6, ~1.3, ~0.8, ~0.3 ka) to as many as nine (if the tentative ~10.0, ~7.0, and ~5.5 ka are considered) local maxima during the MIS 1 or Holocene (Figure 5b). These identified periods are based on overlapping clusters of p-IR $IRSL_{225}$ single-grain ages from multiple samples from distinct nested alluvial fan surfaces (Figure 2). We also notice the repeated overlapping ages between FMM-subpopulations in younger samples and the most recent depositional ages of older samples, producing sharp local maxima (Figures 5b, A2b). These observed overlapping FMM ages suggest that partial bleaching may not be significant in most of our samples (Saha et al., *in press*). Drawing the argument from Saha et al. (*in press*), we therefore argue that some of the K-feldspar single grains in our samples are likely unbleached during the transport. They retain information on the ages of previously well-bleached populations. Thus, we can use the data to infer the timing of past significant sediment depositions.

We compare the upstream depositional periods at the upper Mission Creek alluvial fans with the downstream floodplain deposits on the Banning strand of the SAF at the lower Mission Creek catchment (Figure 5a, b; Saha et al. in prep., Saha et al., *in press*). At least six corresponding depositional periods are identified with ± 1σ standard error during the Holocene (MIS 1) between the upstream and downstream segments (~10 m distance) of the catchment. The downstream depositional periods are identified at ~11.4, ~6.9, ~5.5, ~3.6, ~3.0, ~2.4, ~1.6 (tentatively ~1.2),

and ~0.6 ka (Saha et al., *in press*). This close correspondence between the depositional events inferred from multiple samples from different stratigraphic units and geomorphic landforms in the catchment is highly encouraging. Further, it strengthens our argument that the single-grain FMM-subpopulation ages can be used to infer the timing of most recent and past significant sediment depositions (e.g., Saha et al., *in press*).

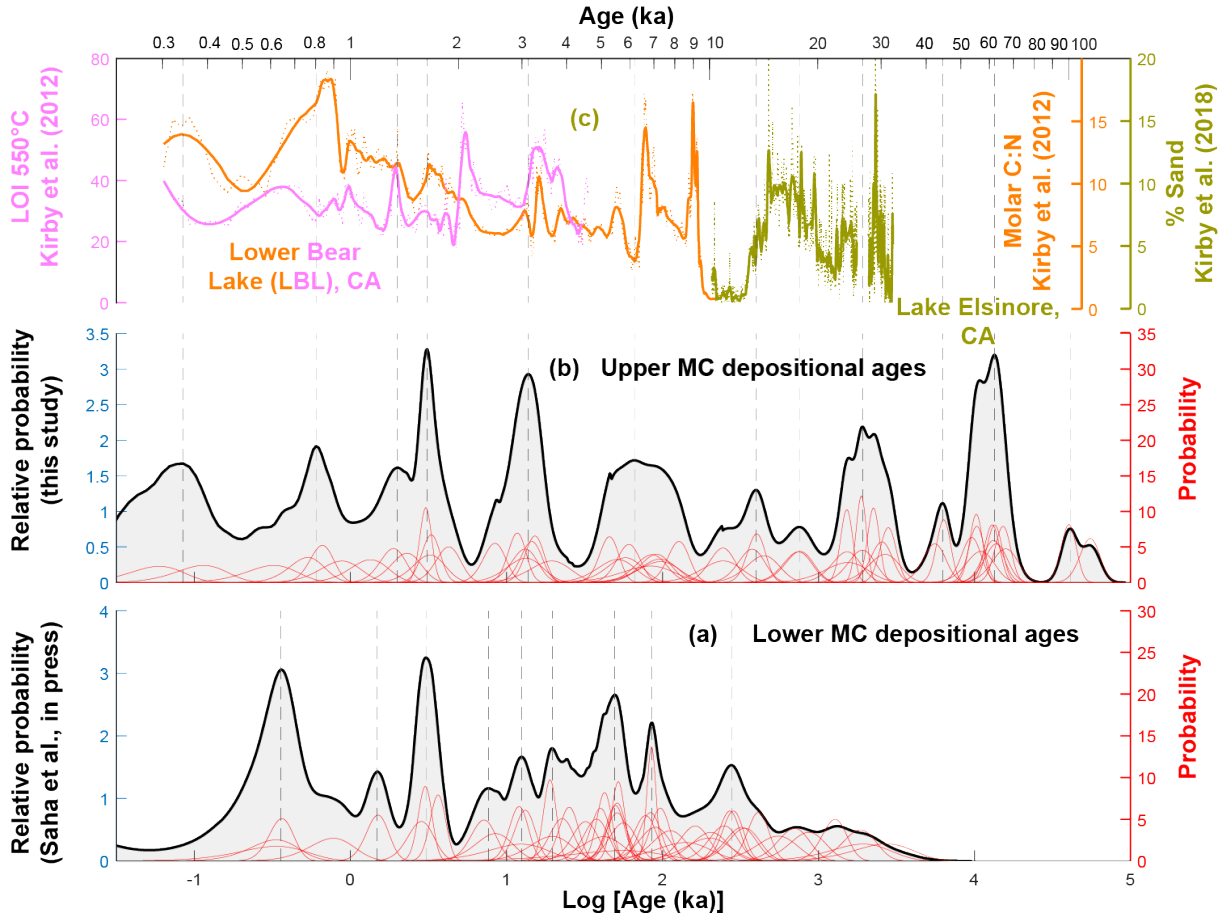

Figure 5. *Comparison between the upper and lower Mission Creek catchment depositional periods and regional hydroclimatic proxies.* ***(a)*** *The probability distribution of lower Mission Creek single-grain subpopulation ages derived using the FMM (Saha et al., in press). (b) The probability distribution of upper Mission Creek single-grain subpopulation ages derived using the same procedure (this study). The individual subpopulation and their relative cPDF distribution are shown in red and black lines, respectively. The probability is shown for age (ka) in the natural log scale (Galbraith, 2011; see section 2.3). At least eight prominent local maxima are identified from the relative cPDF at the lower Mission Creek and twelve from the upper Mission Creek deposits, with at least six common Holocene local maxima in both. These local maxima likely represent the timing of major depositional periods (modal ages are shown in gray dash lines). The hydroclimatic proxies are selected from the nearby terrestrial* ***(c)*** *sites. These include* ***(c)*** *Lower Bear Lake (Kirby et al., 2012, 2015) and Lake Elsinore (Kirby et al., 2018). The original and smoothed variations*

of proxy values are shown in dotted and solid lines, respectively. The ages of all proxies are adjusted to start from AD 2018, consistent with our depositional ages.

When compared with the regional hydroclimatic proxies (Figure 5c), we find a reasonable correspondence between the timing of major depositional periods and the periods of wetter than average late Pleistocene and Holocene hydroclimatic conditions in southern California over sub-millennial to millennial timescales (Kirby et al., 2010, 2012, 2013, 2015; Du et al., 2018). Previous studies have shown a generally wetter hydroclimatic condition in the Late Pleistocene (e.g., ~35–25 ka and ~20–13 ka) and Early Holocene (e.g., ~11.7–7.5 ka) than the Mid- and Late Holocene in southern California (Figure 5c; Bird & Kirby, 2006; Kirby et al., 2015). During the Mid- and Late Holocene, several short-term punctuated intervals of wetter than average conditions are reported (Figure 5c; Negrini et al., 2006; Kirby et al., 2018, 2019; Du et al., 2018). These brief Mid- and Late Holocene wetter intervals are recorded widely in terrestrial lake cores in southern California that include, e.g., the increased molar C:N and total organic matter (LOI 550°C) from Lower Bear Lake (Figure 5c; Kirby et al., 2012), increased % sand from Lake Elsinore (Kirby et al., 2018, 2019), Zaca Lake (Kirby et al., 2014), and Dry Lake (Bird & Kirby, 2006), increased % clay from Silver lake (Kirby et al., 2015), and decreased tufa δ18O from the Salton Sea (Li et al., 2008). In addition, these Mid- and Late Holocene intervals are also recorded in lake highstands from Tulare Lake (Negrini et al., 2006), offshore sediment core data showing increased flood magnitudes and frequency from the Santa Barbara Basin (Du et al., 2018), and sediment accumulation rates from the Hueneme and Newport submarine fans (Romans et al., 2009; Covault et al., 2010; Pigati et al., 2014). Since these brief wetter intervals correspond reasonably well with our observed deposition periods, we think that the intensification of precipitation-related runoff may be responsible for significant sediment deposition in southern California (Benson et al., 2002; Bird & Kirby, 2006; Kirby et al., 2007, 2019; Bird et al., 2010; Glover et al., 2017). Note that we have not yet compared the ~100.8, ~62.1, and ~44.5 ka depositional periods with any hydroclimatic proxies but expected to be also climatically influenced during the MIS 5, 4, and 3, respectively.

Among the proxies used, the significant late Pleistocene (including late glacial) and Holocene depositional periods inferred from luminescence ages, especially at ~26.6, ~17.8, ~13.5, ~6.9–6.2, ~5.5–5.4, ~3.1–3.0, ~1.6, ~0.8, and ~0.3 ka, shows the best match with the wetter periods determined by % sand from the Lake Elsinore and molar C:N and LOI 550°C from the Lower Bear Lake sediment cores in the San Bernardino Mountains (Figure 5). These two proxies are the most proximal to our study site (~50–80 km) and possibly have a similar sensitivity to environmental perturbations.

The work presented here is based on simple assumptions and has some limitations. First, since there is no direct way to quantify the dose rate history experienced by a sample, we assume that the past variability in environmental dose rate is within the uncertainty of the measured dose rates (e.g., Saha et al., *in press*). In addition, we also use assumed internal K of 12.5±0.5 wt.% and measured field water content. To assess these geologic uncertainties, we previously performed a Monte Carlo simulation at the lower Mission Creek site (Saha et al., *in press*) to estimate the ages

based on the range of measured dose rates (i.e., ~4.9–6.4 Gy/ka), assumed internal K (~10–12.5 wt.%; Huntley & Baril, 1997; Smedley 2012; Smedley & Pierce, 2016), and varying water contents (5–20%). Saha et al.'s (*in press*) results showed that the majority (~68–72%) of the simulated ages lie within 20% of the original ages estimated from constant dose rate, assumed internal K, and measured water content. These estimates are expected to be similar in the upper Mission Creek. We expect that the differences are roughly within the 1σ error for most Holocene and late Pleistocene ages (e.g., Saha et al., *in press*). Thus, we argue that this assumption has a negligible impact on our inferred depositional periods.

Second, sedimentation at our trench site could be affected by significant earthquakes in the region (Saha et al., *in press*). Shaking would be expected to produce mass wasting in the steeper terrain upstream of the site, perhaps increasing sediment load in subsequent precipitation events. However, the remobilization and transportation of significant materials from upstream to downstream require sufficient precipitation. Due to the limitations associated with the precision of single-grain luminescence ages and lack of seismically induced independent sediment flux data from the catchment, we are unable to distinguish sedimentation related to seismicity from climate variability and change (Saha et al., *in press*).

Third, luminescence residuals in feldspar grains may introduce age overestimation in some young grains (Li & Li, 2011; Gliganic et al., 2017; Brill et al., 2018). We did not correct this measurement uncertainty.

Lastly, our depositional records are likely incomplete. This could be the product of temporary changes in sediment routing upstream or perhaps erosional events not recognized in the pits and trench exposures (e.g., Holbrook & Miall, 2020). For instance, prominent wetter intervals were recorded around ~9.3–8.5 and ~4.8–4.0 ka, specifically in Lower Bear Lake (Figure 5c) and in Tulare Lake shoreline data (~9.6–8.1 ka; Negrini et al., 2006). Interestingly, no local maxima are identified around these times in the relative cPDF plots at both upper and lower Mission Creek catchment (Figure 5a, b). Similarly, additional peaks are highly likely in the upper Mission Creek at ~10, ~7, and ~5.5 ka (Figure 5b) and are prominent in the lower Mission Creek data (e.g., ~11.4, ~6.9, and ~5.5 ka in Figure 5a). However, relative cPDF could not resolve those peaks due to their overlapping nature (mathematical limitation). Since we cannot directly distinguish well-, poor-, and partially bleached grains in each of our samples, some grains in these periods may be partially bleached and introduced more scatter in ages, which may have reduced the clarity of the age clusters. It is also possible that erosion or no significant deposition occurred around these periods. Similar studies in the region would help resolve this issue. However, we argue that this effect is likely negligible in most of our identified peaks, given the tight age clusters (Saha et al., *in press*).

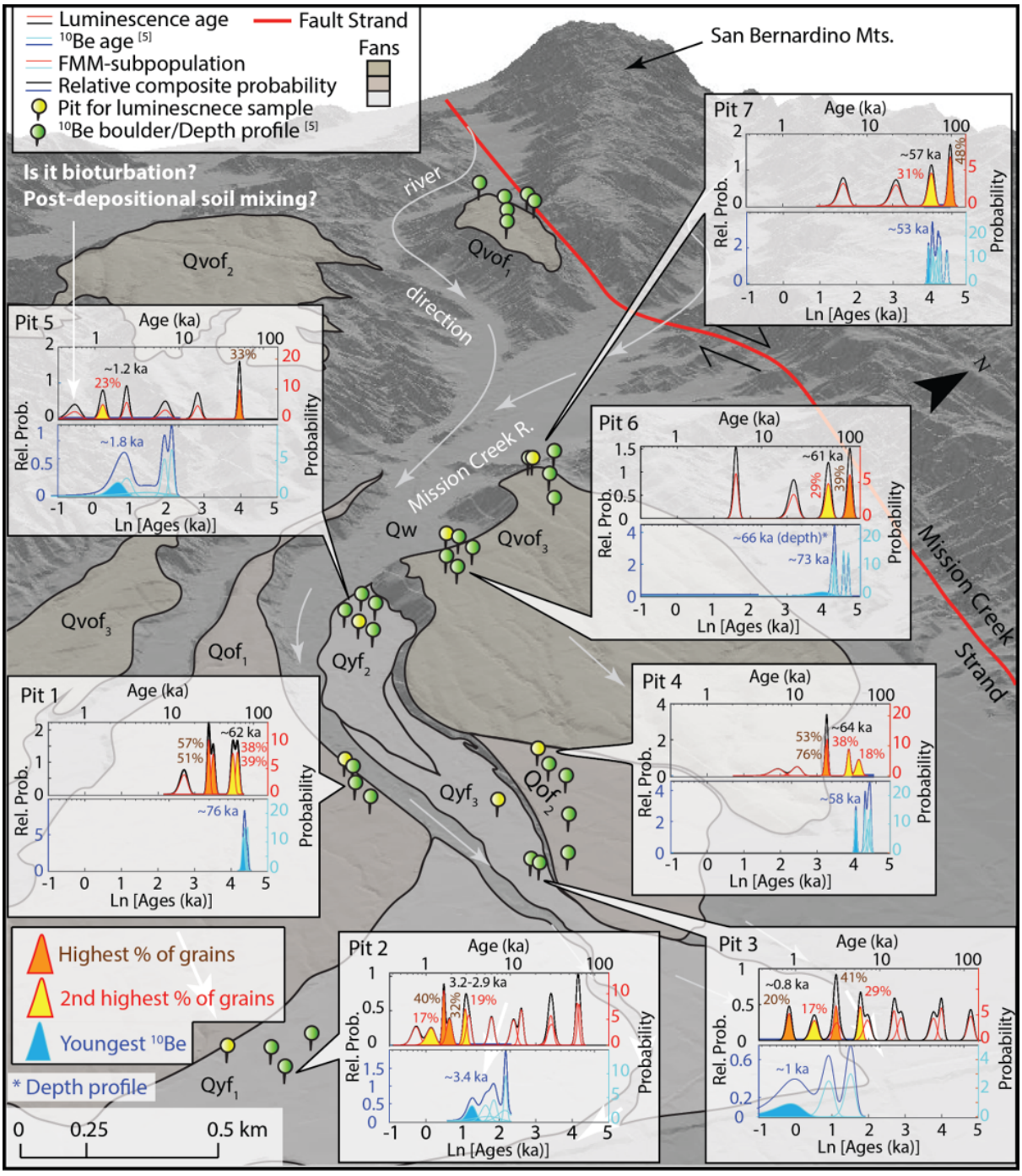

Figure 6. *Triangular irregular networks (TIN) surface map showing the upper Mission Creek catchment's geomorphic setting and eight sub-sequences of the alluvial fans. Probability density plots in a log scale (log[Age (ka)]) showing the luminescence single-grain subpopulation ages from 12 samples and 41 published ^{10}Be ages (Owen et al., 2014). Luminescence subpopulation ages are derived using the FMM. For most fans, FMM-subpopulation ages (burial ages) with the 2nd highest proportion of grains correspond well with the youngest cluster of ^{10}Be ages (i.e., the surface abandonment ages).*

4.2. Sediment reworking and mixing

When compared with the published (recalculated) ^{10}Be ages of the youngest cluster of alluvial fan surface boulders and a depth profile (e.g., surface abandonment ages; D'Arcy et al., 2019), we notice several young FMM-subpopulations in older fan deposits. This is true for all but the youngest (~1–0.8 ka) Holocene fan (Qyf_3). This suggests that the youngest FMM age or the minimum age model (MAM) may not always represent the true surface burial age of the fan but may potentially reflect the age of the recently reworked sediments. Similar findings are also reported for the Qof_1 fan by Ataee (2019) in their independent study from the fan exposure at ~20-m depth from the fan surface. Similar to their results, we also found that the FMM-subpopulations with a higher proportion of single-grains are likely better representative of the burial age of the fan surface. In contrast, the younger FMMs with a lower percentage of single-grains are possibly reworked surface deposits.

In the past few decades, numerous geochronometers were proposed to date geomorphic surfaces (e.g., alluvial fans). These geochronometers include surface exposure dating techniques based on cosmogenic radionuclides (^{10}Be, ^{26}C, ^{14}C), U-series dating of pedogenic carbonates, ^{14}C dating on detrital organic matter, and luminescence dating for quartz and feldspar grains. Unfortunately, there is no perfect dating method. The uncertainties in these methods often produce inaccurate and/or imprecise ages for geomorphic surfaces. For example, ^{10}Be dating on alluvial fan surfaces suffers extensively from reworking, inheritance, and exhumation (e.g., Owen et al., 2014; D'Arcy et al., 2019). In contrast, single grain luminescence can provide evidence of most recent and past burial events but requires a better understanding of the site-specific geomorphic processes to provide an accurate burial age (e.g., Saha et al., *in press*). These outstanding geochronologic uncertainties may be resolved if multiple independent geochronometers are combined. The upper Mission Creek telescopic alluvial fans provide a perfect setting to develop these multiple geochronometic assessments. This study also highlights the strength and uncertainties of the single-grain luminescence dating in these semi-arid alluvial fan and flood plain settings. Caution therefore must be exercised when dating paleoearthquake events and estimating slip rate using alluvial fan deposits and only a single geochronologic method.

5. Conclusions

Our study shows that luminescence ages of single-grain subpopulations can be used to infer the sediment depositional history beyond the most recent depositional periods. We identified at least twelve significant Quaternary depositional periods at ~100.8, ~62.1, ~44.5, ~26.6, ~17.8, ~13.5, ~6.2, ~3.1, ~1.6, ~1.3, ~0.8, and ~0.3 ka in the upper Mission Creek catchment. Of these depositional periods, six corresponding Holocene depositional periods (e.g., ~13.5–11.4, ~6.9–6.2, ~3.6–3.1, ~1.6, ~1.3–1.2, ~0.8–0.6 ka) are identified between the upper and lower Mission Creek, indicating the widespread nature of these significant depositional periods. The close correspondence between the upstream and the downstream luminescence single-grain ages also suggests well-connected storage reservoirs and a more efficient sediment routing system in the

catchment (e.g., Gray et al., 2018, 2019). These depositional periods also indicate that climate, especially the late Pleistocene and Holocene intervals of wetter than average climate, likely plays the first-order control on sediment deposition over the millennial timescale in southern California (e.g., Akciz & Arrowsmith, 2013). Sediment deposition probably occurred as intermittent pulses, primarily controlled by regional and local hydroclimatic variations (e.g., Burt & Allison, 2010; Allen, 2017; Caracciolo et al., 2020). This study also shows that reworking and grain mixing at older (>1 ka) alluvial fan surfaces up to ~1-m-depth is pervasive and must be considered when dating alluvial deposits from these semi-arid fans near the surface using luminesce method. Therefore, our work has important implications for tectonic or paleoclimatic studies that rely on stratigraphic completeness, especially in terrestrial settings (e.g., Washburn et al., 2003; Le Béon et al., 2018), and must be considered when interpreting the fault slip rates or paleoclimatic events in southern California.

APPENDIX 1 – LUMINESCENCE AGE ANALYSIS

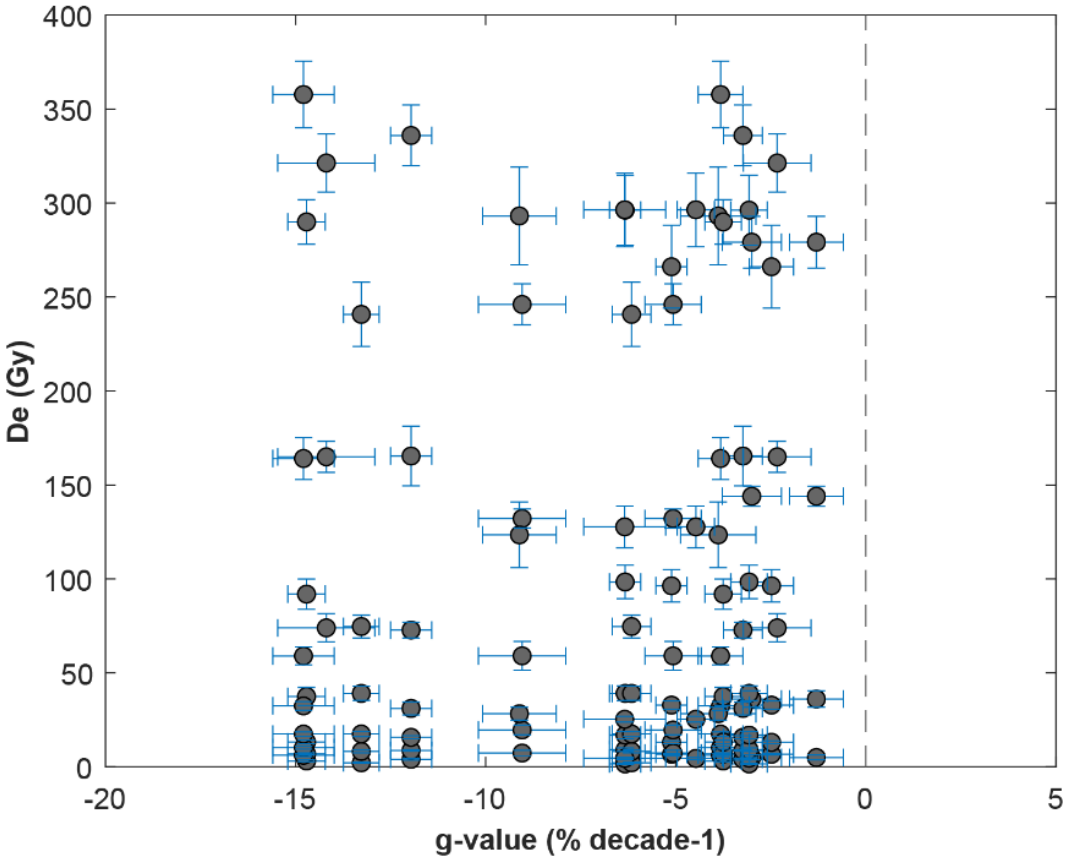

Figure A1. *g-values (% per decade) vs. the equivalent doses (De [Gy]) with 1σ errors showing the fading results on twelve samples. No significant athermal fading is measured during laboratory timescale (300 sec to 4 days) in all samples. Thus, no further correction is made to single-grain p-*

IR IRSL ages. We did not observe any significant fading in the samples measured at 225°C (Fig. 4).

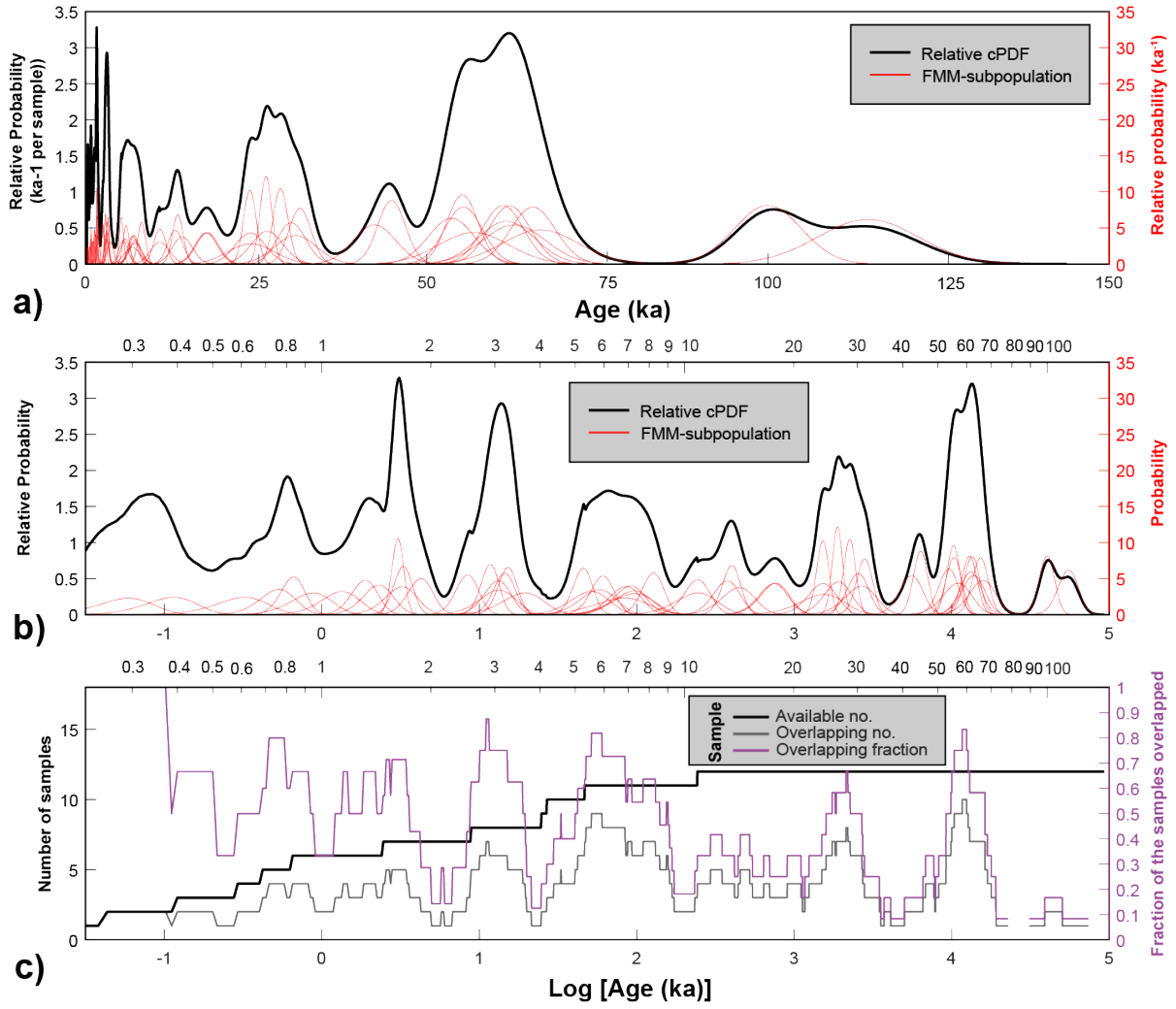

Figure A2. *Sixty FMM-subpopulations are shown, individually in red and their relative cPDF in black, both in linear* ***(a)*** *and log scales* ***(b)****.* ***(c)*** *The number of samples that can provide the record (i.e., available samples) is shown in black for each age interval. The number of samples whose 2σ range overlap (i.e., overlapping samples) is shown in gray and the fraction of overlapping samples relative to available samples is shown in purple for each age interval.*

ACKNOWLEDGMENTS

We acknowledge the support from U.S. Geological Survey under Grant No. G20AP00044. We thank to Ed Rhodes for insightful discussions. SS thanks M. Argueta and R. Missel for helping in the field and C. Kitamikado for help in the UCLA luminescence lab.

PROJECT DATA

The project data include annotated maps, figures, and single-grain post-Infrared Infrared Stimulated Luminescence (p-IR IRSL) ages that constrain the ages of the alluvial fan deposits in the upper Mission Creek catchment. All the processed data will be submitted to a peer-reviewed article and supplementary materials. The raw data will be achieved on Zenodo open-access repository. Reanayzed data for the lower Mission Creek catchment on the Banning strand (that was originally part of the USGS grant # G18A00040 and G18A00041) will be published in GRL soon (https://www.essoar.org/doi/10.1002/essoar.10506324.1). The raw data for that manuscript has already been achieved on Zenodo open-access repository (https://doi.org/10.5281/zenodo.4737624).

BIBLIOGRAPHY OF PUBLICATIONS RESULTING FROM THE WORK PERFORMED UNDER THIS AWARD

Saha, S., Moon, S., Brown, and N.D., Rhodes. In preparation. Examining sediment reworking, transport, and depositional characteristics using single-grain luminescence at the Mission Creek catchment, southern California. Intend to submit to Geology or Geophysical Research Letter.

Saha, S., Moon, S., Brown, N.D., Rhodes, Scharer, K.M., McPhillips, D., McGill, S. F., and Castillo, B. A. 2021 (in press). Holocene depositional history inferred from single-grain luminescence ages in southern California, North America. Geophysical Research Letter

Castillo, B., McGill1, S.F., Scharer, K.M., Yule, J.D., McPhillips, D., McNeil, J., Saha, S., Brown, N.D., and Moon, S. 2021. Ages of Prehistoric Earthquakes on the Banning Strand of the San Andreas Fault, near North Palm Springs, California. Geosphere 17, 1–26.

Saha, S., Moon, S., Brown, N.D., and Rhodes, E. 2020. Examining single-grain luminescence dating uncertainties between upstream fans and downstream sediment deposits in the seismically active southern California. 2020 AGU Fall meeting, Online. EP029-0008.

Saha, S., S. Moon, N. Brown, and E. Rhodes, 2019, Inferring sediment dynamics using single-grain feldspar post-IR IRSL luminescence dating in southern California, North America: American Geophysical Union, Fall 2019 meeting, Paper GC13A-06.

Saha, S., S. Moon, N. D. Brown, E. J. Rhodes, S. F. McGill, B. A. Castillo, K. M. Scharer, D. McPhillips, and D. Yule, 2019, Influence of sediment dynamics and alluvial fan formation on paleoseismic studies in southern California, North America: Southern California Earthquake Center 2019 Annual Meeting, poster #129.

REFERENCES

Akçiz, S. O., & Arrowsmith, J. R. (2013). New views on the evolution of the San Andreas fault zone in central California and the Carrizo Plain. Field Guide 32, *Geological Society of America, 1–12.*

Allen, P.A. (2017). Sediment Routing Systems. The Fate of Sediments from Source to Sink. *Cambridge University Press,* Cambridge. https://doi.org/10.1017/9781316135754.

Armitage, J. J., Duller, R. A., Whittaker, A. C., & Allen, P. A. (2011). Transformation of tectonic and climatic signals from source to sedimentary archive. *Nature Geoscience, 4(4),* 231–235. https://doi.org/10.1038/ngeo1087

Armitage, J. J., Dunkley Jones, T., Duller, R. A., Whittaker, A. C., & Allen, P. A. (2013). Temporal buffering of climate-driven sediment flux cycles by transient catchment response. *Earth and Planetary Science Letters, 369–370,* 200–210. https://doi.org/10.1016/j.epsl.2013.03.020

Arnold, L. J., Bailey, R. M., & Tucker, G. E. (2007). Statistical treatment of fluvial dose distributions from southern Colorado arroyo deposits. *Quaternary Geochronology*, *2*(1–4), 162–167. https://doi.org/10.1016/j.quageo.2006.05.003

Ataee, Nina. (2019). Development of luminescence dating methods in tectonically active settings: dating seismic related fanglomerates in alluvial fans located in Coachella Valley, southern California. Master's thesis at Kansas State University, Manhattan, Kansas. https://krex.k-state.edu/dspace/handle/2097/39677

Balco, G., Blisniuk, K., & Hidy, A. 2019. Chlorine-36/beryllium-10 burial dating of alluvial fan sediments associated with the Mission Creek strand of the San Andreas Fault system, California, USA. *Geochronology, 1, 1–16.* https://doi.org/10.5194/gchron-1-1-2019

Bell, W.T. (1980). Alpha dose attenuation in quartz grains for thermoluminescence dating. *Ancient TL, 12,* 4–8.

Benson, S. R., Croll, D. A., Marinovic, B. B., Chavez, F. P., & Harvey, J. T. (2002). Changes in the cetacean assemblage of a coastal upwelling ecosystem during El Niño 1997-98 and La Niña 1999. *Progress in Oceanography, 54(1–4),* 279–291. https://doi.org/10.1016/S0079-6611(02)00054-X

Berger, G. (2010). An alternate form of probability-distribution plots for D.E. values. *Ancient TL, 28(1),* 11–21.

Berger, G. W. (2011). Response to Galbraith. *Ancient TL, 29*, 48–50.

Biasi, G.P., Weldon, R.J., Fumal, T.E., & Seitz, G.G. 2002, Paleoseismic event dating and the conditional probability of large earthquakes on the southern San Andreas Fault, California. *Bulletin of the Seismological Society of America 92, 2761–2781.*

Bird, B. W., & Kirby, M. E. (2006). An alpine lacustrine record of early Holocene North American Monsoon dynamics from Dry Lake, southern California (USA). *Journal of Paleolimnology, 35(1),* 179–192. https://doi.org/10.1007/s10933-005-8514-3

Bird, B. W., Kirby, M. E., Howat, I. M., & Tulaczyk, S. (2010). Geophysical evidence for Holocene lake-level change in southern California (Dry Lake). *Boreas, 39(1),* 131–144. https://doi.org/10.1111/j.1502-3885.2009.00114.x

Bøtter-Jensen, L., McKeever, S. W. S., & Wintle, A. G. (2003). Optically Stimulated Luminescence Dosimetry. *Optically Stimulated Luminescence Dosimetry,* 1–355. https://doi.org/10.1016/B978-0-444-50684-9.X5077-6

Bowman, D. (1978). Determination of intersection points within a telescopic alluvial fan complex. *Earth Surface Processes, 3*, 265–276.

Brandon, Mark T. (1992). Decomposition of fission-track grain-age distributions. *American Journal of Science, 292*, 535–564.

Brennan, B. J., Lyons, R. G., & Phillips, S. W. (1991). Attenuation of alpha particle track dose for spherical grains. *International Journal of Radiation Applications and Instrumentation. Part, 18(1–2)*, 249–253. https://doi.org/10.1016/1359-0189(91)90119-3

Brill, D., Reimann, T., Wallinga, J., May, S. M., Engel, M., Riedesel, S., & Brückner, H. (2018). Testing the accuracy of feldspar single grains to date late Holocene cyclone and tsunami deposits. *Quaternary Geochronology, 48,* 91–103. https://doi.org/10.1016/j.quageo.2018.09.001

Brown, N. D. (2020). Which geomorphic processes can be informed by luminescence measurements? *Geomorphology, 367*, 107296. https://doi.org/10.1016/j.geomorph.2020.107296

Bull, W. B. (1977). The alluvial-fan environment. *Prog. Phys. Geogr. 1*, 222–270.

Bull, W. B. (1991). Geomorphic Responses to Climate Change. *Oxford University Press,* New York.

Bull, W. B. (2000). Correlation of fluvial aggradation events to times of global climate change. *In: Noller, J. S., Sowers, J. M., Lettis, W. R. (eds.), Quaternary Geochronology: Methods and Applications.* American Geophysical Union, Washington, D.C., pp. 456–464.

Burt, T. P., & Allison, R. J. (2010). Sediment cascades. *In: Burt, T. P., Allison, R. J. (eds.), Sediment Cascades in the Environment: An Integrated Approach.* John Wiley and Sons, pp. 1–15.

Buylaert, J. P., Murray, A. S., Thomsen, K. J., & Jain, M. (2009). Testing the potential of an elevated temperature IRSL signal from K-feldspar. *Radiation Measurements, 44(5–6),* 560–565. https://doi.org/10.1016/j.radmeas.2009.02.007

Caracciolo, L., Chew, D., & Andò, S. (2020). Sediment Generation and Sediment Routing Systems. *Earth-Science Reviews, 207.* https://doi.org/10.1016/j.earscirev.2020.103221

Castillo, B., McGill1, S. F., Scharer, K. M., Yule, J. D., McPhillips, D., McNeil, J., Saha, S., Brown, N. D. & Moon, S. (2021). Prehistoric Earthquakes on the Banning Strand of the San Andreas Fault, North Palm Springs, California. *Geosphere 17, 1–26. https://dx.doi.org/10.1130/GES02237.1*

Colarossi, D., Duller, G. A. T., Roberts, H. M., Tooth, S., & Lyons, R. (2015). Quaternary Geochronology Comparison of paired quartz OSL and feldspar post-IR IRSL dose distributions in poorly bleached fluvial sediments from South Africa. *Quaternary Geochronology, 30,* 233–238. https://doi.org/10.1016/j.quageo.2015.02.015

Colombo, F. (2005). Quaternary telescopic-like alluvial fans, Andean Ranges, Argentina. In *Harvey, A. M., Mather, A. E., & Stokes, M. (eds.). Alluvial fans: Geomorphology, sedimentology, dynamics - Introduction. A review of alluvial-fan research. Geological Society Special Publication, 251* (1):69. https://doi.org/10.1144/GSL.SP.2005.251.01.01

Covault, J. A., Romans, B. W., Fildani, A., McGann, M., & Graham, S. A. (2010). Rapid climatic signal propagation from source to sink in a southern California sediment-routing system. *Journal of Geology, 118(3)*, 247–259. https://doi.org/10.1086/651539

D'arcy, M. K., Schildgen, T. F., Turowski, J. M., & Dinezio, P. (2019). Inferring the timing of abandonment of aggraded alluvial surfaces dated with cosmogenic nuclides. *Earth Surface Dynamics, 7(3),* 755–771. https://doi.org/10.5194/esurf-7-755-2019

Du, X., Hendy, I., & Schimmelmann, A. (2018). A 9000-year flood history for Southern California: A revised stratigraphy of varved sediments in Santa Barbara Basin. *Marine Geology 397,* 29–42. https://doi.org/10.1016/j.margeo.2017.11.014

Durcan, J. A., King, G. E., & Duller, G. A. T. (2015). Quaternary Geochronology DRAC : Dose Rate and Age Calculator for trapped charge dating. *Quaternary Geochronology, 28*, 54–61. https://doi.org/10.1016/j.quageo.2015.03.012

Ellwein, A. L., Mahan, S. A., & McFadden, L. D. (2015). Impacts of climate change on the formation and stability of late Quaternary sand sheets and falling dunes, Black Mesa region, southern Colorado Plateau, USA. *Quaternary International*, *362*(March), 87–107. https://doi.org/10.1016/j.quaint.2014.10.015

Fosdick, J. C., & Blisniuk, K. (2018). Sedimentary signals of recent faulting along an old strand of the San Andreas Fault, USA. *Scientific Reports, 8(1)*, 1–10. https://doi.org/10.1038/s41598-018-30622-3

Galbraith, R. (2011) Some comments arising from Berger (2010). *Ancient TL, 29*, 41–47.

Galbraith, R. F. (2005). Statistics for Fission Track Analysis. *Chapman and Hall/CRC*, London.

Galbraith, R. F., & Green, P. F. (1990). Estimating the component ages in a finite mixture. *International Journal of Radiation Applications and Instrumentation. Part, 17(3)*, 197–206. https://doi.org/10.1016/1359-0189(90)90035-V

Galbraith, R. F., & Laslett, G. M. (1993). Statistical models for mixed fission track ages. *International Journal of Radiation Applications and Instrumentation. Part, 21(4)*, 459–470. https://doi.org/10.1016/1359-0189(93)90185-C

Gliganic, L. A., Cohen, T. J., Meyer, M., & Molenaar, A. (2017). Variations in luminescence properties of quartz and feldspar from modern fluvial sediments in three rivers. *Quaternary Geochronology, 41*, 70–82. https://doi.org/10.1016/j.quageo.2017.06.005

Gliganic, L. A., May, J. H., & Cohen, T. J. (2015). All mixed up: Using single-grain equivalent dose distributions to identify phases of pedogenic mixing on a dryland alluvial fan. *Quaternary International, 362(1)*, 23–33. https://doi.org/10.1016/j.quaint.2014.07.040

Gliganic, Luke Andrew, Cohen, T. J., Slack, M., & Feathers, J. K. (2016). Sediment mixing in aeolian sandsheets identified and quantified using single-grain optically stimulated luminescence. *Quaternary Geochronology, 32*, 53–66. https://doi.org/10.1016/j.quageo.2015.12.006

Glover, K. C., MacDonald, G. M., Kirby, M. E., Rhodes, E. J., Stevens, L., Silveira, E., Whitaker, A., & Lydon, S. (2017). Evidence for orbital and North Atlantic climate forcing in alpine Southern California between 125 and 10 ka from multi-proxy analyses of Baldwin Lake. *Quaternary Science Reviews, 167,* 47–62. https://doi.org/10.1016/j.quascirev.2017.04.028

Gray, H. J., Jain, M., Sawakuchi, A. O., Mahan, S. A., & Tucker, G. E. (2019). Luminescence as a Sediment Tracer and Provenance Tool. *Reviews of Geophysics, 57(3)*, 987–1017. https://doi.org/10.1029/2019RG000646

Gray, H. J., Tucker, G. E., Mahan, S. A., & Al, G. E. T. (2018). Application of a Luminescence-Based Sediment Transport Model. *Geophysical Research Letters, 45*, 6071–6080. https://doi.org/10.1029/2018GL078210

Guerin, G., Mercier, N., Nathan, R., Adamiec, C., & Lefrais, Y. (2012). On the use of the infinite matrix assumption and associated concepts: a critical review. *Radiat. Meas. 47,* 778–785. https://doi.org/10.1016/j.radmeas.2012.04.004

Hart, E. W., & Bryant, W. A., compilers. (2001). Fault number 30a, Maacama fault zone, northern section, in Quaternary fault and fold database of the United States: *U.S. Geological Survey website*, https://earthquakes.usgs.gov/hazards/qfaults, accessed 10/12/2020 10:50 AM.

Harvey, A. M., Wigand, P. E., & Wells, S. G. (1999). Response of alluvial fan systems to the late Pleistocene to Holocene climatic transition: Contrasts between the margins of pluvial Lakes Lahontan and Mojave, Nevada and California, USA. *Catena, 36(4)*, 255–281. https://doi.org/10.1016/S0341-8162(99)00049-1

Hempton, M.R., Dunne, L.A., & Dewey, J.F. 1983. Sedimentation in an Active Strike-Slip Basin, Southeastern Turkey. *The Journal of Geology 91, 401–412.*

Holbrook, J. M., & Miall, A. D. (2020). Time in the Rock: A field guide to interpreting past events and processes from siliciclastic stratigraphy. *Earth-Science Reviews, 203*, 103–121. https://doi.org/10.1016/j.earscirev.2020.103121

Huntley, D. J., & Lamothe, M. (2001). Ubiquity of anomalous fading in K-feldspars and the measurement and correction for it in optical dating, *NRC Research Press, 1106*, 1093–1106. https://doi.org/10.1139/cjes-38-7-1093

Huntley, D., & Baril, M. (1997). The K content of the K-feldspars being measured in optical dating or in thermoluminescence dating. *Ancient TL, 15(1)*, 11–13.

Inman, D. L., & Jenkins, S. A. (1999). Climate change and the episodicity of sediment flux of small California Rivers. *Journal of Geology, 107(3)*, 251–270. https://doi.org/10.1086/314346

Ivy-Ochs, S., Kerschner, H., & Schlüchter, C. (2007). Cosmogenic nuclides and the dating of Lateglacial and Early Holocene glacier variations: The Alpine perspective. *Quaternary International, 164–165,* 53–63. https://doi.org/10.1016/j.quaint.2006.12.008

Jerolmack, D. J., & Paola, C. (2010). Shredding of environmental signals by sediment transport. *Geophysical Research Letters, 37(19),* 1–5. https://doi.org/10.1029/2010GL044638

Kendrick, K. J., Matti, J. C., & Mahan, S. A. (2015). Late quaternary slip history of the Mill Creek strand of the San Andreas fault in San Gorgonio Pass, southern California: The role of a subsidiary left-lateral fault in strand switching. *Bulletin of the Geological Society of America, 127(5–6)*, 825–849. https://doi.org/10.1130/B31101.1

Kirby, E., Harkins, N., Wang, E., Shi, X., Fan, C., & Burbank, D. (2007). Slip rate gradients along the eastern Kunlun fault. *Tectonics, 26(2)*, 1–16. https://doi.org/10.1029/2006TC002033

Kirby, M. E., Feakins, S. J., Bonuso, N., Fantozzi, J. M., & Hiner, C. A. (2013). Latest Pleistocene to Holocene hydroclimates from Lake Elsinore, California. *Quaternary Science Reviews, 76,* 1–15. https://doi.org/10.1016/j.quascirev.2013.05.023

Kirby, M. E., Feakins, S. J., Hiner, C. A., Fantozzi, J., Zimmerman, S. R. H., Dingemans, T., & Mensing, S. A. (2014). Tropical Pacific forcing of Late-Holocene hydrologic variability in the coastal southwest United States. *Quaternary Science Reviews, 102*, 27–38. https://doi.org/10.1016/j.quascirev.2014.08.005

Kirby, M. E., Heusser, L., Scholz, C., Ramezan, R., Anderson, M. A., Markle, B., Rhodes, E., Glover, K. C., Fantozzi, J., Hiner, C., Price, B., Rangel, H. (2018). A late Wisconsin (32–10k cal a B.P.) history of pluvials, droughts and vegetation in the Pacific south-west United States (Lake Elsinore, CA). *Journal of Quaternary Science, 33(2)*, 238–254. https://doi.org/10.1002/jqs.3018

Kirby, M. E., Knell, E. J., Anderson, W. T., Lachniet, M. S., Palermo, J., Eeg, H., Lucero, R., Murrieta, R., Arevalo, A., & Silveira, E., Hiner, C. A. (2015). Evidence for insolation and Pacific forcing of late glacial through Holocene climate in the Central Mojave Desert (Silver Lake, CA). *Quaternary Research (United States), 84(2),* 174–186. https://doi.org/10.1016/j.yqres.2015.07.003

Kirby, M. E., Lund, S. P., Patterson, W. P., Anderson, M. A., Bird, B. W., Ivanovici, L., Monarrez, P., & Nielsen, S. (2010). A Holocene record of Pacific Decadal Oscillation (PDO)-related hydrologic variability in Southern California (Lake Elsinore, CA). *Journal of Paleolimnology, 44(3),* 819–839. https://doi.org/10.1007/s10933-010-9454-0

Kirby, M. E., Patterson, W. P., Lachniet, M., Noblet, J. A., Anderson, M. A., Nichols, K., & Avila, J. (2019). Pacific southwest United States Holocene droughts and pluvials inferred from sediment $18^{\delta}O$ (calcite) and gran size data (Lake Elsinore, California). *Frontiers in Earth Science, 7:74,* 1–14.

Kirby, M. E., Zimmerman, S. R. H., Patterson, W. P., & Rivera, J. J. (2012). A 9170-year record of decadal-to-multi-centennial scale pluvial episodes from the coastal Southwest United States: A role for atmospheric rivers? *Quaternary Science Reviews, 46*, 57–65. https://doi.org/10.1016/j.quascirev.2012.05.008

Kreutzer, S., Schmidt, C., Fuchs, M. C., Dietze, M., & Fuchs, M. (2012). Introducing an R package for luminescence dating analysis, *30(1)*, 1–8.

Lancaster, J.T., Hayhurst, C.A., and Bedrossian, T.L., compilers, (2012). Preliminary Geologic Map of Quaternary Superficial Deposits in Southern California Palm Springs 30′×60′ Quadrangle: *California Geological Survey Special Report, 217*, Plate 24, scale 1:100,000. https://www.conservation.ca.gov/cgs/publications/sr217

Le Béon, M., Tseng, Y. C., Klinger, Y., Elias, A., Kunz, A., Sursock, A., Daëron, M., Tapponnier, P., Jomaa, R. (2018). High-resolution stratigraphy and multiple luminescence dating techniques to reveal the paleoseismic history of the central Dead Sea fault (Yammouneh fault, Lebanon). *Tectonophysics, 738–739*, 1–15. https://doi.org/10.1016/j.tecto.2018.04.009

Li, B., & Li, S. (2011). Quaternary Geochronology Luminescence dating of K-feldspar from sediments: A protocol without anomalous fading correction. *Quaternary Geochronology, 6*, 468–479. https://doi.org/10.1016/j.quageo.2011.05.001

Li, H. C., Xu, X. M., Ku, T. L., You, C. F., Buchheim, H. P., & Peters, R. (2008). Isotopic and geochemical evidence of palaeoclimate changes in Salton Basin, California, during the past 20 kyr: 1. $\delta^{18}O$ and $\delta^{13}C$ records in lake tufa deposits. *Palaeogeography, Palaeoclimatology, Palaeoecology, 259(2–3)*, 182–197. https://doi.org/10.1016/j.palaeo.2007.10.006

Liritzis, I. (2013). Luminescence Dating in Archaeology, Anthropology, and Geoarchaeology: An Overview (Springer Briefs in Earth System Sciences). Springer.

Matti, J. C., Morton, D. M., & Langenheim, V. E. (2015). Geologic and geophysical maps of the El Casco 7.5′ quadrangle, Riverside County, southern California, with accompanying geologic-map database: *U.S. Geological Survey Open-File Report 2010–1274, 141* p., 3 sheets, scale 1:24,000. https://doi.org/10.3133/ofr20101274.

Matti, J.C., and Cossette, P.M., 2007, Classification of surficial materials, Inland Empire Region, southern California: conceptual and operational framework: *U.S. Geological Survey, Open-File Report (in progress)*.

McGuire, C., & Rhodes, E. J. (2015). Downstream MET-IRSL single-grain distributions in the Mojave River, southern California: Testing assumptions of a virtual velocity model. *Quaternary Geochronology, 30*, 239–244. https://doi.org/10.1016/j.quageo.2015.02.004

Miall, A. D. (2015). Updating uniformitarianism: stratigraphy as just a set of 'frozen accidents.' *In: Smith, D. G., Bailey, R. J., Burgess, P. M., Fraser, A. J. (eds.), Strata and Time: Probing the Gaps in Our Understanding. Geological Society*, London, Special Publications, pp. 404.

Miller, D. M., Schmidt, K. M., Mahan, S. A., McGeehin, J. P., Owen, L. A., Barron, J. A., Lehmkuhl, F., Löhrer, R. (2010). Holocene landscape response to seasonality of storms in the Mojave Desert. *Quaternary International, 215(1–2)*, 45–61. https://doi.org/10.1016/j.quaint.2009.10.001

Murray, A. S., & Wintle, A. G. (2000). Luminescence dating of quartz using an improved single-aliquot regenerative-dose protocol. *Radiation Measurements, 32(1)*, 57–73. https://doi.org/10.1016/S1350-4487(99)00253-X

Negrini, R. M., Wigand, P. E., Draucker, S., Gobalet, K., Gardner, J. K., Sutton, M. Q., & Yohe, R. M. (2006). The Rambla highstand shoreline and the Holocene lake-level history of Tulare Lake, California, USA. *Quaternary Science Reviews, 25(13–14)*, 1599–1618. https://doi.org/10.1016/j.quascirev.2005.11.014

Owen, L. A., Clemmens, S. J., Finkel, R. C., & Gray, H. (2014). Late Quaternary alluvial fans at the eastern end of the San Bernardino Mountains, Southern California. *Quaternary Science Reviews, 87*, 114–134. https://doi.org/10.1016/j.quascirev.2014.01.003

Pigati, J. S., Rech, J. A., Quade, J., & Bright, J. (2014). Desert wetlands in the geologic record. *Earth-Science Reviews, 132,* 67–81. https://doi.org/10.1016/j.earscirev.2014.02.001

Ponti, D. J. (1985). The quaternary alluvial sequence of the antelope valley, California. *Special Paper of the Geological Society of America, 203,* 79–96. https://doi.org/10.1130/SPE203-p79

Prescott, J. R., & Hutton, J. T. (1994). Cosmic ray contributions to dose rates for luminescence and ESR dating: Large depths and long-term time variations. *Radiation Measurements, 23(2–3)*, 497–500. https://doi.org/10.1016/1350-4487(94)90086-8

Reimann, T., Thomsen, K. J., Jain, M., Murray, A. S., & Frechen, M. (2012). Single-grain dating of young sediments using the pIRIR signal from feldspar. *Quaternary Geochronology, 11*, 28–41. https://doi.org/10.1016/j.quageo.2012.04.016

Rhodes, E. J. (2011). Optically Stimulated Luminescence Dating of Sediments over the Past 200,000 Years. *Annual Review of Earth and Planetary Sciences, 39,* 461–488 https://doi.org/10.1146/annurev-earth-040610-133425

Rhodes, E. J. (2015). Dating sediments using potassium feldspar single-grain IRSL: Initial methodological considerations. *Quaternary International, 362,* 14–22. https://doi.org/10.1016/j.quaint.2014.12.012

Romans, B. W., Castelltort, S., Covault, J. A., Fildani, A., & Walsh, J. P. (2016). Environmental signal propagation in sedimentary systems across timescales. *Earth-Science Reviews, 153,* 7–29. https://doi.org/10.1016/j.earscirev.2015.07.012

Romans, B. W., Normark, W. R., McGann, M. M., Covault, J. A., & Graham, S. A. (2009). Coarse-grained sediment delivery and distribution in the Holocene Santa Monica Basin, California: Implications for evaluating source-to-sink flux at millennial time scales. *Bulletin of the Geological Society of America, 121(9–10)*, 1394–1408. https://doi.org/10.1130/B26393.1

Saha, S., Moon, S., Brown, and N.D., Rhodes. In prep. Examining sediment reworking, transport, and depositional characteristics using single-grain luminescence at the Mission Creek catchment, southern California.

Saha, S., Moon, S., Brown, N.D., Rhodes, Scharer, K.M., McPhillips, D., McGill, S. F., and Castillo, B. A. (2021, in press). Holocene depositional history inferred from single-grain luminescence ages in southern California, North America. Geophysical Research Letter, in print.

Smedley, R. K. & Pearce, N. J. G. (2016). Internal U, Th and Rb concentrations of alkali-feldspar grains: Implications for luminescence dating. *Quaternary Geochronology, 35,* 16–25.

Smedley, R. K., Duller, G. A. T., & Roberts, H. M. (2015). Bleaching of the post-IR IRSL signal from individual grains of K-feldspar: Implications for single-grain dating. *Radiation Measurements, 79*, 33–42. https://doi.org/10.1016/j.radmeas.2015.06.003

Smedley, R. K., Duller, G. A. T., Pearce, N. J. G., Roberts, H. M. (2012). Determining the K-content of single-grains of feldspar for luminescence dating. *Radiation Measurements, 47(9),* 790–796.

Spelz, R. M., Fletcher, J. M., Owen, L. A., & Caffee, M. W. (2008). Quaternary alluvial-fan development, climate and morphologic dating of fault scarps in Laguna Salada, Baja California, Mexico. *Geomorphology, 102(3–4),* 578–594. https://doi.org/10.1016/j.geomorph.2008.06.001

Toby, S. C., Duller, R. A., De Angelis, S., & Straub, K. M. (2019). A Stratigraphic Framework for the Preservation and Shredding of Environmental Signals. *Geophysical Research Letters, 46(11),* 5837–5845. https://doi.org/10.1029/2019GL082555

Wallinga, J. (2002). Optically stimulated luminescence dating of fluvial deposits: A review. *Boreas, 31(4),* 303–322. https://doi.org/10.1080/030094802320942536

Warrick, J. A., & Milliman, J. D. (2003). Hyperpycnal sediment discharge from semi-arid southern California rivers: implications for coastal sediment budgets. *Geology 31,* 781–784.

Washburn, Z., Arrowsmith, J. R., Dupont-Nivet, G., Wang, X. F., Zhang, Y. Q., & Chen, Z. (2003). Paleoseismology of the Xorxol Segment of the Central Altyn Tagh Fault, Xinjiang, China. *Annals of Geophysics, 46(5)*, 1015–1034. https://doi.org/10.4401/ag-3443

Wells, S. G., McFadden, L. D., & Dohrenwend, J. C. (1987). Influence of late Quaternary climatic changes on geomorphic and pedogenic processes on a desert piedmont, Eastern Mojave Desert, California. *Quaternary Research, 27(2),* 130–146. https://doi.org/10.1016/0033-5894(87)90072-X

Wells, S. G., McFadden, L. D., & Harden, J. (1990). Preliminary results of age estimations and regional correlations of Quaternary alluvial fans within the Mojave Desert in southern California. *In: Reynolds, R. E., Wells, S. G., Brady, R. H. (eds.), At the End of the Mojave—Quaternary Studies in the Eastern Mojave Desert. San Bernardino County Museum Association, Redlands, California*, pp. 45–54.